

SCALE EFFECT ON SHEAR STRENGTH OF COMPUTER-AIDED-MANUFACTURED JOINTS

Tzou-Shin Ueng¹, Yue-Jan Jou², and I-Hui Peng³

ABSTRACT

In order to systematically study the scale effect on the shear strength of rock joints, this study used the computer-aided-manufacturing system to reproduce the artificial rock joints for Barton's standard joint profiles of $JRC = 4 \sim 6$ and $18 \sim 20$, natural rock joint profiles, and saw-toothed joints. We divided, enlarged, reduced, and assembled these joint profiles to obtain joint specimens of various sizes ranging from 75 mm to 300 mm in length. Direct shear tests were conducted on these joint specimens to obtain the peak shear strengths under different normal stresses. The surface conditions of the joints at failure were also examined. Based on the test results in this study, it was found that the joint surface geometry configuration rather than the specimen size itself is the main factor in the scale effect on the peak shear strength of rock joints. The geometry configuration or roughness of each individual joint should be evaluated in the use of empirical relations to compute the shear strengths of rock joints of various sizes.

Key words: Rock joints, shear strength, scale effect, computer-aided-manufacture, shear tests.

1. INTRODUCTION

There exists a scale effect on the strength of rock materials, including rock masses, intact rocks, fractured rocks and rock joints. The scale effect on the peak shear strength of rock joints has been studied previously by many researchers. They usually divided a large natural or artificially reproduced rock joint specimen into various smaller sizes of rock joints. Direct shear tests under a given normal stress were then conducted on these rock joints of various sizes. The scale effect on the peak shear strength was then obtained empirically by comparing the average peak shear strength of rock joints of each specimen size to that of the original larger specimen. The relations thus obtained represented the trend of changes for overall average values of shear strengths in a rather wide scattered range. Based on results of a large amount of shearing tests, Barton and his co-workers (Barton and Choubey 1977; Bandis *et al.* 1981; Barton and Bandis 1982) proposed an empirical equation to estimate the peak shear strength (τ_p) of a rock joint:

$$\tau_p = \sigma_n \tan \left[JRC \log \left(\frac{JCS}{\sigma_n} \right) + \phi_b \right] \quad (1)$$

where σ_n = normal stress on the joint surface, JRC = joint roughness coefficient, JCS = joint wall compression strength, and ϕ_b =

basic friction angle. They considered the scale effect on the shear strength using:

$$JRC_n = JRC_o \left[\frac{L_n}{L_o} \right]^{-0.02JRC_o} \quad (2)$$

$$JCS_n = JCS_o \left[\frac{L_n}{L_o} \right]^{-0.03JRC_o} \quad (3)$$

where L_o = laboratory joint size (nominal 100 mm), L_n = in situ joint size, JRC_o and JCS_o = JRC and JCS values for the laboratory specimen size, and JRC_n and JCS_n = JRC and JCS values for the in situ joint size. According to Eqs. (1), (2) and (3), the peak shear strength of rock joint decreases with increasing joint size. Others also developed various size-dependent characterizations for rock joint surface roughness (*e.g.*, Fardin *et al.* 2001; Murata and Saito 2003) by the similar approach. Meso and macro constitutive modeling for scale effect on the shear strength of rock joints was carried out by Vallier *et al.* (2005).

In fact, the scale effect of the peak shear strength of a rock joint surface includes the effects of specimen size itself and the geometry configuration of the joint surface. It is not uncommon that the scale effect on peak shear strengths of many particular rock joints does not follow the average trend of size effect for the combination of all rock joints with different roughness and surface geometries. It was found in some studies that the shear strength of joints decreased with increasing specimen size (*e.g.*, Pratt *et al.* 1974; Giani *et al.* 1992), while in other cases, the strength increased with specimen size (*e.g.*, Giani *et al.* 1992; Brown *et al.* 1977). In these previous studies, the variations of roughness and geometry configurations of the joint surface profiles of different specimen sizes were not thoroughly considered in the empirical correlation. The geometry characteristics or the roughness of a divided smaller joint surface could be quite different from that of the original larger joint surface. On the other

Manuscript received June 25, 2010; revised August 30, 2010; accepted August 31, 2010.

¹ Professor Emeritus (corresponding author), Department of Civil Engineering, National Taiwan University, Taipei 10617, Taiwan; Technical Advisor, National Center for Research on Earthquake Engineering, 200, Sect. 3, Hsinhai Rd., Taipei 10668, Taiwan, R.O.C. (e-mail: ueng@ntu.edu.tw).

² Former graduate student, Department of Civil Engineering, National Taiwan University, Taipei 10617, Taiwan, R.O.C.

³ Director, Strategy and Marketing, CoreTech System (Modex3D) Co., 8F-2, No. 32, Taiyuan St., Chupei City, Hsinchu County 302, Taiwan, R.O.C.

hand, is the *JRC* value of an enlarged or reduced joint surface profile (in both horizontal and vertical directions) the same as that of the original one or does it change according to Eq. (2)? Therefore, without fully understanding of the true affecting factors and the mechanism of the scale effect on the peak shear strength, these empirical relations, *e.g.*, Eqs. (1), (2) and (3), can only be used for preliminary rough estimate of shear strengths of various sizes of rock joints, but are not suitable for more accurate modeling or theoretical analysis.

In order to clarify the aforementioned concerns, different sizes of rock joint specimens with systematically varying geometry configurations of the joint surface profiles are made using a computer-aided-manufacturing (CAM) system. The effects of size and geometry on the peak shear strength of rock joints are evaluated according to the results of direct shear tests on these rock joint surfaces.

2. COMPUTER-AIDED-MANUFACTURED JOINT SPECIMENS

This study only considered a two-dimensional geometrical profile along the length, *i.e.*, in the shearing direction of the joint specimen. The upper and lower joint surfaces are matched as for a tension joint. The size of a specimen is determined based on the length, rather than the area, of the joint specimen. The width of the specimen was kept at 100 mm for all different sizes of specimens. The size and geometry of the joint surface were systematically varied for the study of the effect of geometry and size on the peak shear strength of the rock joint. In this study, the geometries of the original joint surface profiles included the flat smooth surface, triangular saw-toothed surfaces (including sym-

metrical 15° and 30° slopes with a tooth-base length of 20 mm), Barton's typical joint roughness profiles ($JRC = 4 \sim 6$ and $18 \sim 20$), and Nankang sandstone natural joint surface ($JRC \approx 10 \sim 12$ comparing to Barton's typical profiles). The original joint surface profiles were digitized and saved as electronic files. We considered 3 types of geometry configurations of joint surface profiles, which can be easily produced using the computer software (Chang 1999; Huang 2000):

1. Division of a 300 mm profile into 1/2, 1/3, and 1/4 of the original length. Figure 1 shows an example of the division of the Barton's typical profile of $JRC = 18 \sim 20$.
2. Enlargement of a 100-mm profile by 2 and 3 times, or reduction of a 300-mm profile by 1/3 and 2/3 proportionally in length and height. Figures 2 and 3 show examples of the joint profile enlargement and reduction, respectively.
3. Assembly of two or three repeated 100-mm profiles into joints of 2 or 3 times the original profile length as shown in Fig. 4.

Table 1 shows the joint surface profiles tested in this study. Except the flat smooth joint surface, the simulated joint surface was first produced as a Rapid Prototype (RP) model using the HELISYS's LOM1015-PLUS laminated object manufacturing system in the CAM Laboratory, National Taiwan University. This system used a laser to cut a special type of paper (0.1 mm in thickness) into the prescribed shape controlled by the computer, and these sheets of paper were then glued together to become a solid RP model joint as shown in Fig. 5. This joint surface was used to cast the mould for the lower-half joint surface with silicon rubber (RTV-533) as the mould material. This mould was then used to cast the lower joint specimens and, in turn, the mould for the upper-half joint specimens.

Table 1 Joint surface profiles tested in this study

Original profile	Geometry variation	Length, mm
Flat smooth	Basic friction	100, 200, 300
Barton's $JRC = 4 \sim 6$	Divide the enlarged 300-mm Barton's profile into 1/2 and 1/3	100, 150, 300
Barton's $JRC = 18 \sim 20$	Divide the enlarged 300-mm Barton's profile into 1/2 and 1/3	75, 100, 150, 300
Natural joint	Divide the original 300-mm natural joint into 1/2 and 1/3	100, 150, 300
Saw tooth, 15° and 30° slopes, base = 20 mm	Enlarge the 100-mm profile by 2 and 3 times	100, 200, 300
Barton's $JRC = 4 \sim 6$	Enlarge the 100-mm typical profile by 2 and 3 times	100, 200, 300
Barton's $JRC = 18 \sim 20$	Enlarge the 100-mm typical profile by 2 and 3 times	100, 200, 300
Natural joint	Reduce the original profile by 1/2 and 1/3	100, 200, 300
Barton's $JRC = 4 \sim 6$	Enlarge a 100-mm divided section by 2 and 3 times	100, 200, 300
Barton's $JRC = 18 \sim 20$	Enlarge a 100-mm divided section by 2 and 3 times	100, 200, 300
Natural joint	Enlarge a 100-mm divided section by 2 and 3 times	100, 200, 300
Barton's $JRC = 4 \sim 6$	Assembly of 2 and 3 repeated 100-mm typical profiles	100, 200, 300
Barton's $JRC = 18 \sim 20$	Assembly of 2 and 3 repeated 100-mm typical profiles	100, 200, 300
Saw tooth, 15° and 30° slopes, base = 20 mm	Assembly of 2 and 3 repeated 100-mm profiles	100, 200, 300

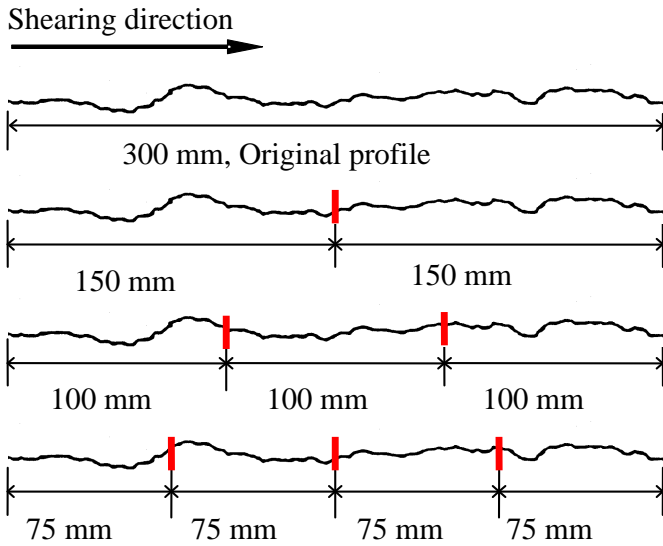


Fig. 1 Division of Barton's $JRC = 18 \sim 20$ profile

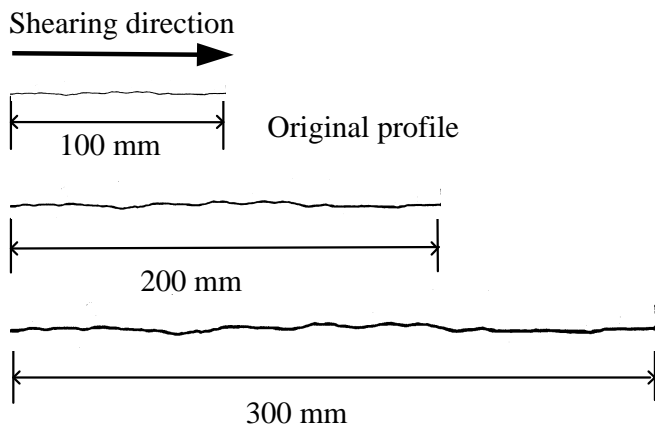


Fig. 2 Enlargement of Barton's $JRC = 4 \sim 6$ profile

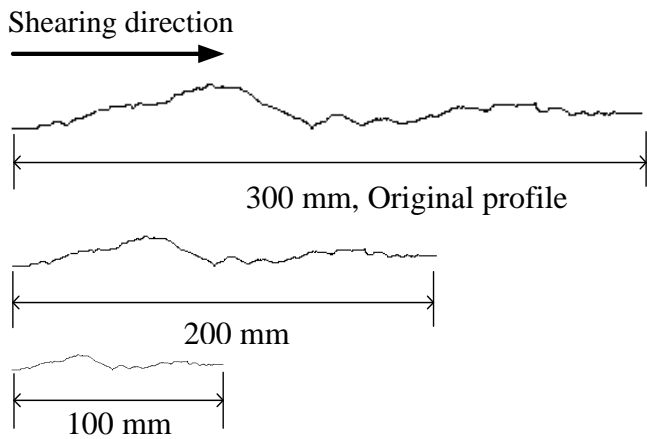


Fig. 3 Reduction of a natural joint profile

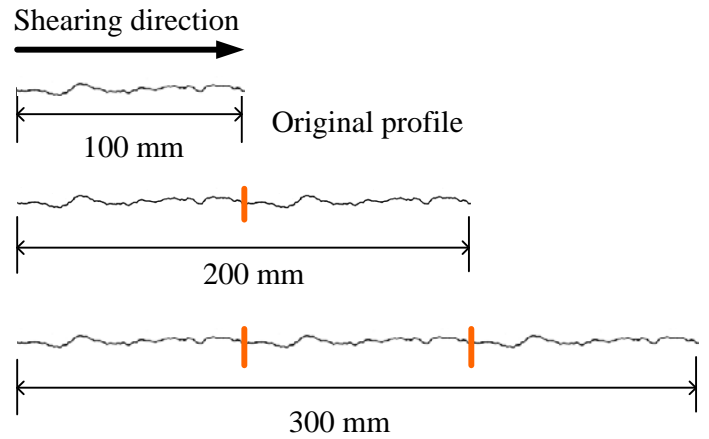


Fig. 4 Assembly of repeated Barton's $JRC = 18 \sim 20$ profiles



Fig. 5 Rapid prototype models

The flat smooth joints were obtained by saw-cutting a $300 \text{ mm} \times 100 \text{ mm} \times 150 \text{ mm}$ joint material into the desired specimen sizes and the surfaces were polished with #120 sandpaper before direct shear tests.

The casting material for the joint specimens consisted of a mixture of plaster of Paris, silica powder (#606), and water (1 : 0.75 : 1 by weight). The specimen was kept in a room of a temperature at $26 \sim 30^\circ\text{C}$ and a relative humidity of $50 \sim 70\%$ for a curing time of four weeks before testing in order to obtain consistent material properties for different specimen sizes. The unconfined compressive strength of the material ranged from 9.0 MPa for a specimen of 54-mm in diameter to 6.8 MPa for a specimen of 162-mm in diameter. However, in the direct shear tests on the intact material, there was no significant difference in the peak shear stresses at failure under a given normal stress for specimens with lengths ranging from 75 mm to 200 mm as shown in Fig. 6. Therefore, differing from Eq. (3) for the unconfined compressive strength, it is considered that there is insignificant size effect on the shear strength under direct shearing for the joint material used in this study.

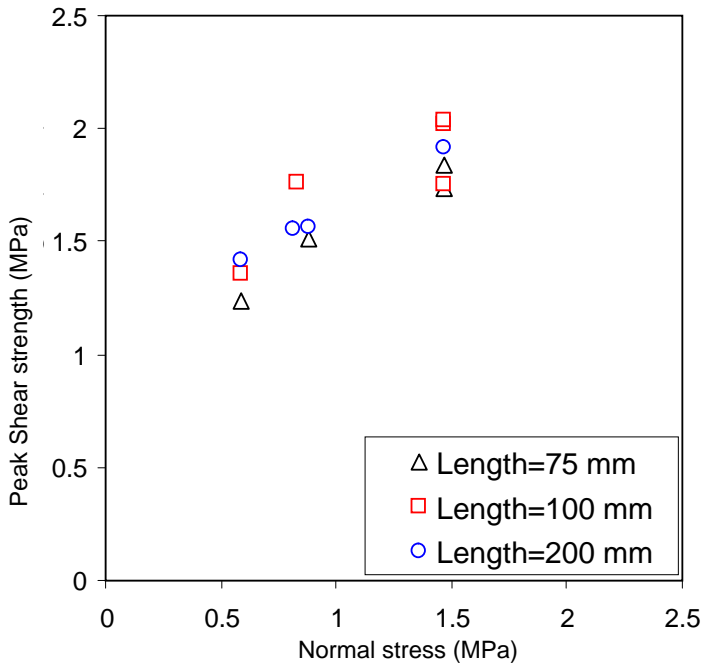


Fig. 6 Peak shear stress at failure for the intact specimen material

3. DIRECT SHEAR TESTS ON JOINT SPECIMENS

The direct shear tests on the joint specimens were performed using a 100-kN direct shear test apparatus capable of testing a specimen of up to 300×300 mm in cross section with a maximum shear displacement of 500 mm under a servo-controlled normal force of up to 100-kN. The machine was modified to provide the free dilation of the upper half of the joint specimen, to better constrain the rotation of the specimen, and to minimize the friction between the upper and lower shear boxes during shearing tests (Peng 2001). The tests were conducted following mostly the procedures given in the ISRM "Suggested method for laboratory determination of direct shear strength" (ISRM 1981). The shearing rate was controlled at 0.5 mm/min. During the shearing tests, normal forces, normal displacements, shear forces, and shear displacements were measured and recorded by a data acquisition system. The peak shear strength of the joint was the maximum shear stress during the shear test. Owing to the large joint specimen sizes and the limitation of the equipment loading capacity, the applied normal stress conditions in this study only represent those usually encountered in civil engineering projects concerning rock slope stability and excavations in a shallow ground compared to the much higher normal stresses involved in the deep mining.

After each test, surface conditions of both upper and lower halves of the joint specimen were examined. Locations and distribution of the damaged areas due to crushing, shearing, tearing and other causes (they are called "failure areas" in this paper) on the upper and lower joint surfaces were then marked as shown in Fig. 7 (the dark colored areas are the intact surfaces and the light areas are the damaged surfaces) and the total failure area on each joint surface could be calculated accordingly.

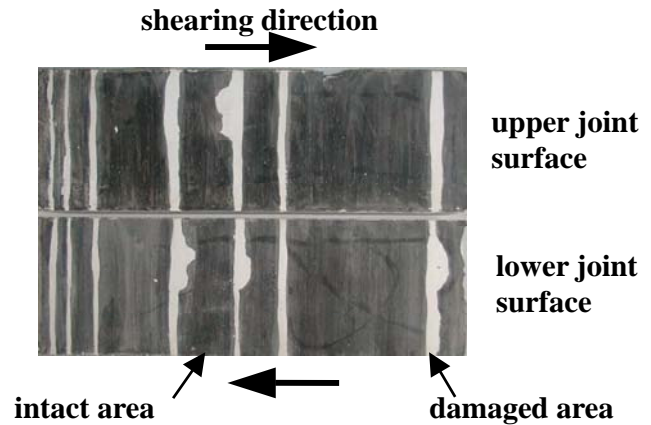


Fig. 7 Marked joint surface conditions after failure

4. PEAK SHEAR STRENGTH TEST RESULTS

4.1 Basic Friction Angle

Figure 8 shows the results of the basic friction tests on the flat smooth joint specimens with lengths of 100 mm, 200 mm, and 300 mm. The basic friction angle is about 35° regardless of the specimen size. Apparently, there is no scale effect on the basic friction angle of flat smooth joint surfaces.

4.2 Divided Joint Surfaces

The relation of peak shear strength of divided joint specimen versus specimen length is given in Fig. 9. The test results show that the strengths of most individual smaller divided joints are higher than that of the larger original joint; but some smaller joints exhibit lower strengths than that of the larger joint. For a rougher ($JRC = 18 \sim 20$) original joint surface, there is an obvious "positive" scale effect on the average peak shear strength of divided joint specimens, *i.e.*, the "average" peak shear strength decreases with increasing specimen size. However, for the smoother ($JRC = 4 \sim 6$) and natural original joints ($JRC \approx 10 \sim 12$), there is only a slight scale effect on the peak shear strength of divided joint specimens. Similar findings were also obtained by Bandis *et al.* (1981) and Ohnishi and Herda (1993).

Figure 10 shows the surface conditions after shear tests for the original and divided natural joint specimens. It can be seen that the failure areas on divided smaller joint surfaces are similar to those of the same corresponding parts of the original large joint surface. However, some divided joint surfaces show different damage patterns of small asperities, probably leading to scattering of the peak strengths of these specimens.

It appeared that the geometry configuration or roughness of a divided smaller joint surface could be quite different from that of the original larger joint surface. Therefore, for the calculation of peak shear strength of a rock joint, besides the specimen size, the geometry of the joint surface profile should be re-evaluated for each individual divided joint specimen rather than regardlessly using Eqs. (2) and (3).

4.3 Enlarged and Reduced Joint Surfaces

For these proportionally enlarged and reduced joint surfaces, we consider their geometric configurations the same for different

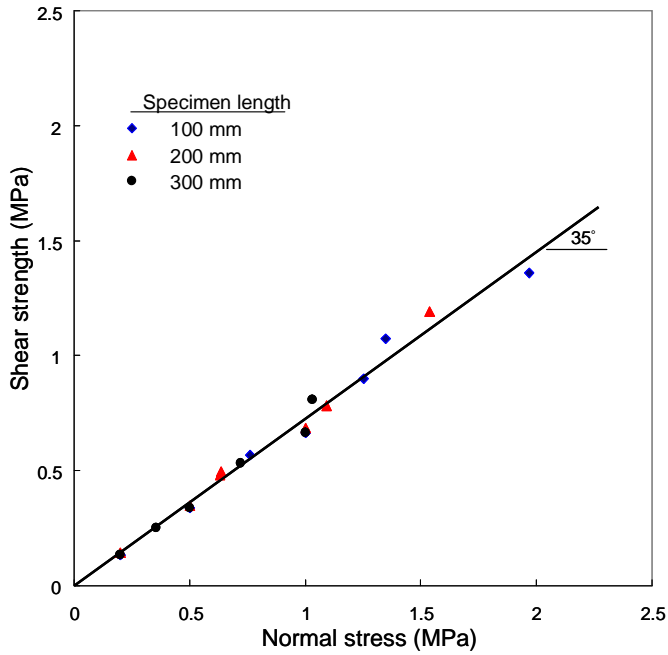
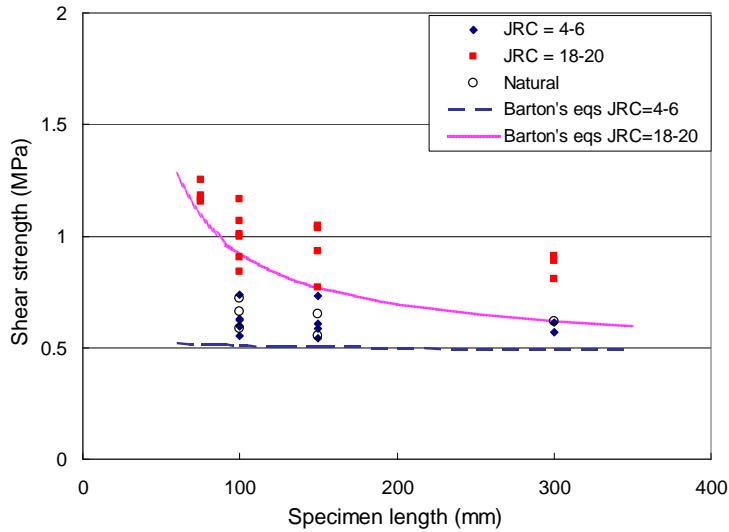
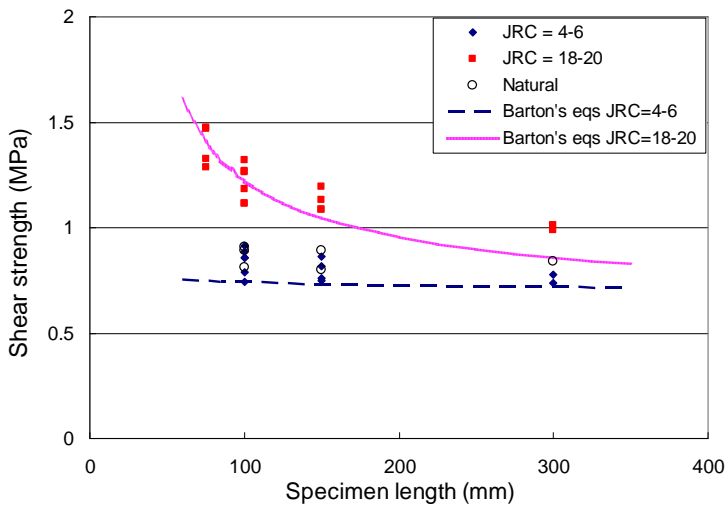


Fig. 8 Results of basic friction tests on the flat smooth joints

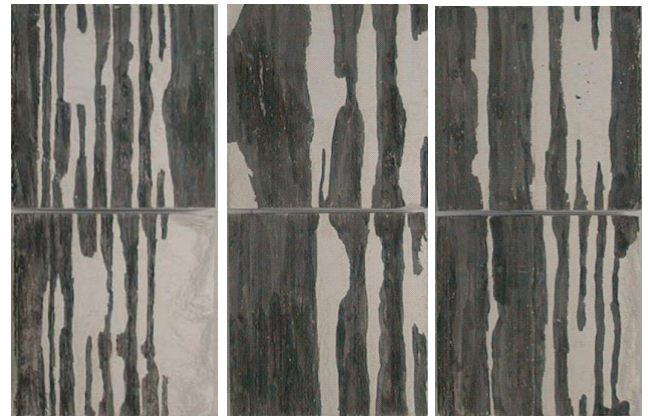


(a) $\sigma = 0.588$ MPa



(b) $\sigma = 0.882$ MPa

Fig. 9 Peak shear strengths of divided joints versus specimen length



(a) 1/3 division, specimen length = 100 mm



(b) 1/2 division, specimen length = 150 mm



(c) original joint profile, specimen length = 300 mm

Fig. 10 Surface conditions after shear tests for the divided natural joint specimens under normal stress = 0.882 MPa

specimen sizes. Figure 11 shows the test results of the peak shear strengths of the enlarged and reduced joint specimens versus specimen length. It can be seen that for joint specimens of proportionally enlarged or reduced surface profiles in both length and height, there is no definite trend of change for the shear strength against the specimen length. No significant difference was found for the peak shear strengths and the sheared surface areas of joint specimens of different sizes under the same normal stress. Ohnishi and Yoshinaka (1992) also found the similar results for regular tooth joints with specimen lengths ranging from 30 mm to 120 mm.

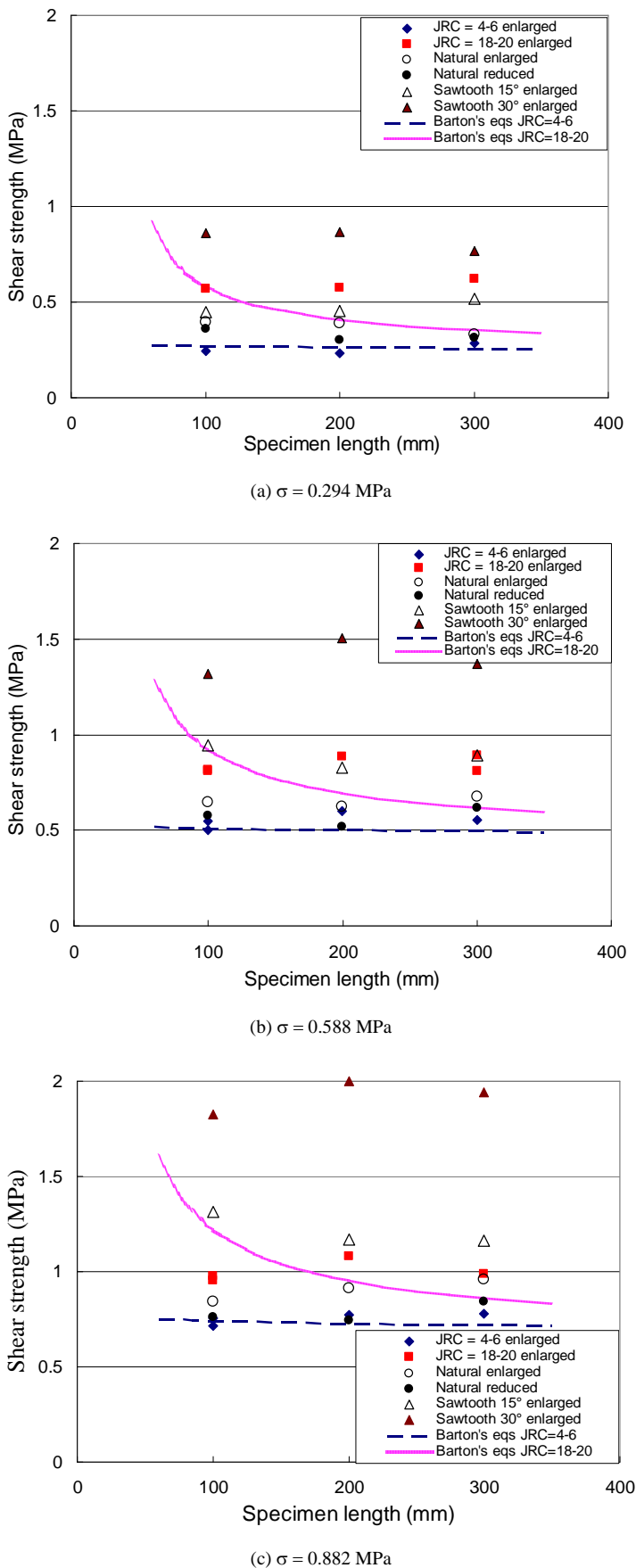


Fig. 11 Peak shear strengths of enlarged and reduced joints versus specimen length

The surface conditions after shearing, as shown in Fig. 12, indicate that the locations and sizes of the failure areas are similar for different enlarged and reduced specimen lengths. The same geometry configurations of these joint surfaces might be the reason. Therefore, there is no significant scale effect for rock joints with the same geometry configuration.

4.4 Assembly of Repeated Joint Surfaces

According to Fig. 13, for a smoother $JRC = 4 \sim 6$ surface profile, there is little difference in the peak shear strengths of joint specimens of different assembly sizes under the same normal stress, whereas for the rougher, $JRC = 18 \sim 20$, and saw-toothed surface profiles, the peak shear strength of the 100-mm specimens is slightly higher than those of 200-mm and 300-mm specimens. The shear strengths of specimens of the latter two sizes are essentially the same. Similar results were also found by Ohnishi and Herda (1993).

For this type of joint specimens, even though the geometry of each joint segment is identical, the assembly of more than one joint segment exhibits a geometry configuration differing from that of the individual segment. Examination of the joint surface conditions after shear tests (Fig. 14) reveals that most of the surface damage patterns are similar, but not identical, on each individual segment of the original profile which was put together to form the assembled joint specimen. There are some differences in the details of the damage conditions among these individual parts.

4.5 Discussions on Test Results

The relations, Eqs. (1), (2) and (3), developed by Barton and his co-workers are also plotted on Figs. 9, 11 and 13 for $JRC = 4 \sim 6$ and $18 \sim 20$ to compare with the test results. The values of parameters used in the computations are: $L_o = 100$ mm, $\phi_b = 35^\circ$, and $JCS_o = 9.0$ MPa. For the divided joint specimens (Fig. 9), the Barton's relations correspond to the trend of variation of the tested peak shear strength versus joint length, except that these relations under-predicted the peak shear strength for the larger joint specimens. However, the test results for the enlarged, reduced, and assembled joint specimens (Figs. 11 and 13) do not fit well the Barton's relations. It is interesting to note that the scale effect relations obtained by Barton and others were developed mostly based on the results of shearing tests on specimens divided from larger joint specimens, but not on the proportionally enlarged or reduced rock joints.

After evaluating the specimen sizes, the geometry configurations and the peak shear strengths for various types of joint specimens presented in the previous Subsections, it can be concluded that the peak shear strength of a rock joint is mainly affected by the geometry configuration rather than the specimen size.

Besides the effect of geometry configuration, the differences of the peak shear strength between small and large joint specimens might possibly be caused by the fact that the match and contact between the upper and lower surfaces for the longer joints were more likely not as good as that for the smaller individual joints, and the peak shear stress usually occurred at a larger displacement for the larger joint specimen, which in turn changed the dilatancy during shearing. In addition, the normal stress on the larger joint surface may be less uniformly distributed over the whole joint area. However, these would not affect the overall trend of scale effect on the peak shear strength of joints obtained in this study.



(a) original joint length = 100 mm



(b) joint length = 200 mm

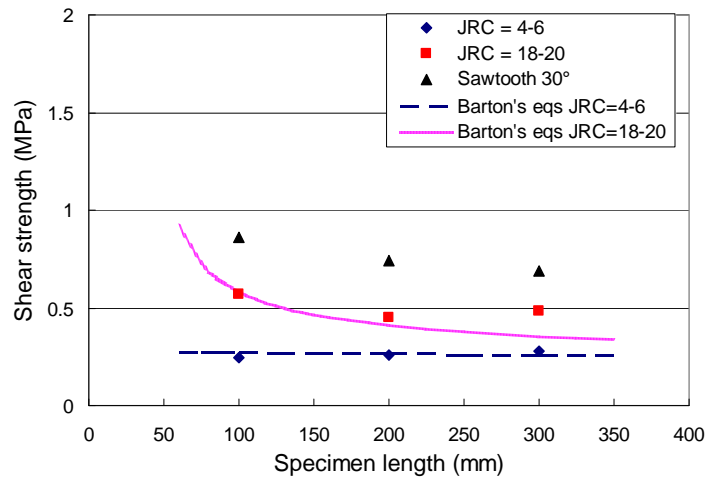


(c) joint length = 300 mm

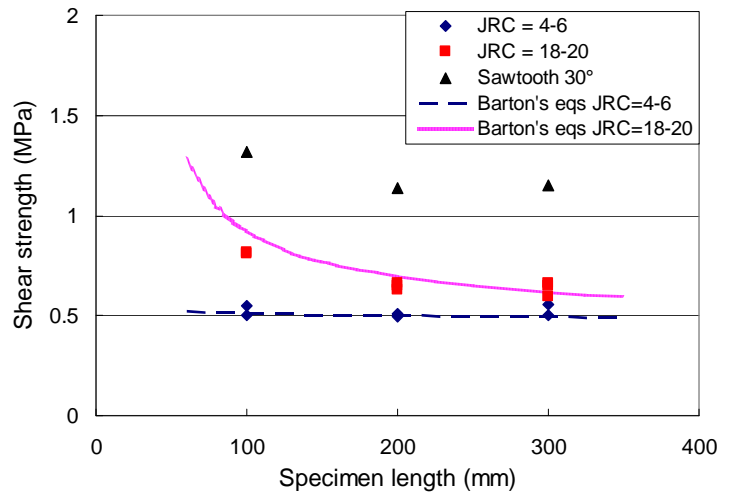
Fig. 12 Joint surface conditions after shear tests for enlarged joint specimens ($JRC = 18 \sim 20$) under normal stress = 0.588 MPa

5. FAILURE AREAS OF JOINT SURFACE AFTER SHEAR TESTS

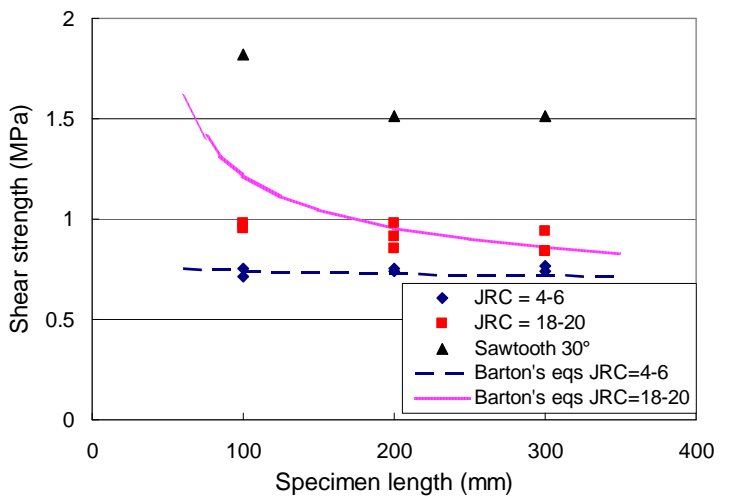
The photographs of the marked joint surfaces after shear tests were digitized and the areas of the damaged and sheared-off parts (failure areas) of the upper and lower joint surfaces of each joint specimen were then computed accordingly. The percentage of the failure areas against the whole joint surface area was calculated for each joint specimen according to:



(a) $\sigma = 0.294$ MPa



(b) $\sigma = 0.588$ MPa



(c) $\sigma = 0.882$ MPa

Fig. 13 Peak shear strengths of assembly of repeated joint surfaces



(a) original joint length = 100 mm



(b) 2 x Joint length = 200 mm



(c) 3 x Joint length = 300 mm

Fig. 14 Joint surface conditions after shear test for assembled joint specimens ($JRC = 18 \sim 20$) under normal stress = 0.588 MPa

failure area (%)

$$= \frac{\text{sum of failure areas on the upper and lower joint surfaces}}{\text{total joint surface areas of the upper and lower joint surfaces}} \times 100\% \quad (4)$$

As expected, the failure area percentage increases with increasing normal stress. For example, Fig. 15 is the test results for

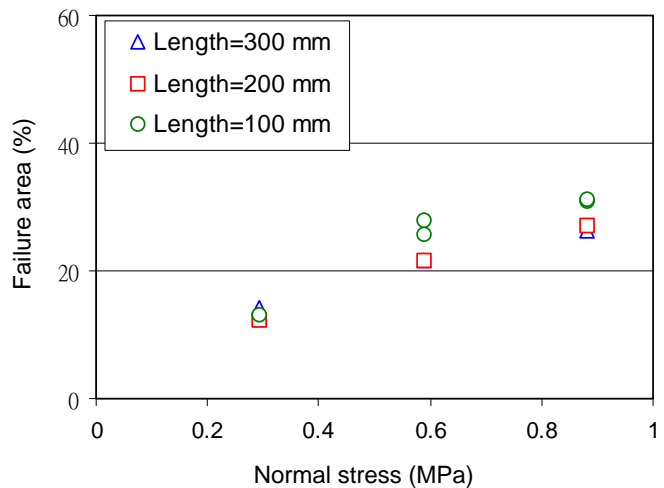


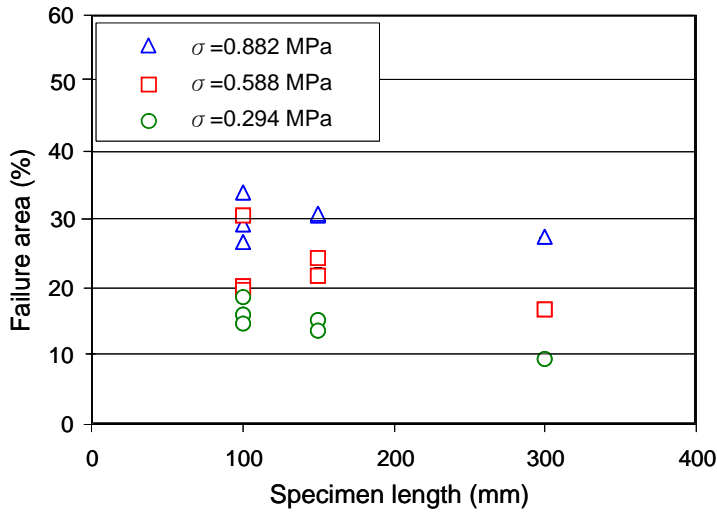
Fig. 15 Failure area percentage versus normal stress for various sizes of enlarged joint specimens ($JRC = 4 \sim 6$)

the enlarged joint profiles with $JRC = 4 \sim 6$. It was found, according to the test results, that there is no definite trend of change of failure area percentage versus change of specimen size, except that for the nature joint specimens. Figure 16 shows that failure area percentage decreases with increasing joint specimen size for the natural joint surface in various test conditions. However, the changes of the failure areas on the joint surfaces do not generally correspond to the change of the peak shear strength versus specimen size as indicated in Section 4.

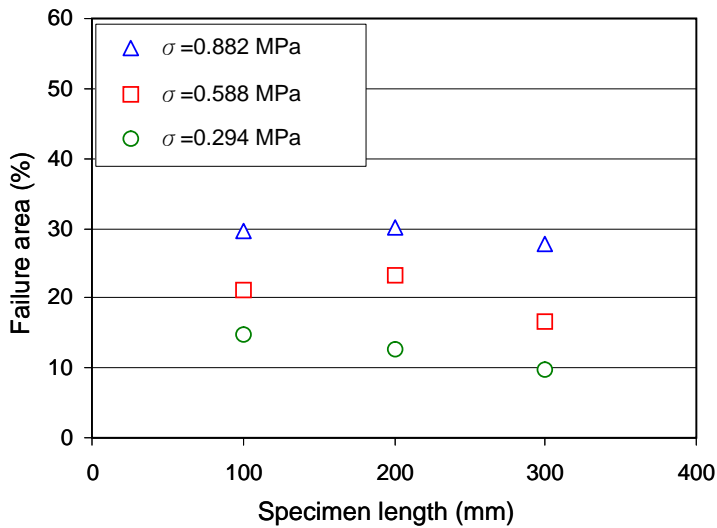
6. CONCLUSIONS

Rock joint specimens with systematically varied sizes and geometry configurations were made using a computer-aided-manufacturing system. Joint specimens of various sizes ranging from 75 mm to 300 mm in length were obtained by dividing, enlarging, reducing, and assembling various types of joint profiles. Direct shear tests on these joint specimens were performed under normal stresses usually encountered in civil engineering projects for rock slopes and excavations in a shallow depth. The effects of size and geometry on the peak shear strength of these rock joints were evaluated. The results obtained in this study show that:

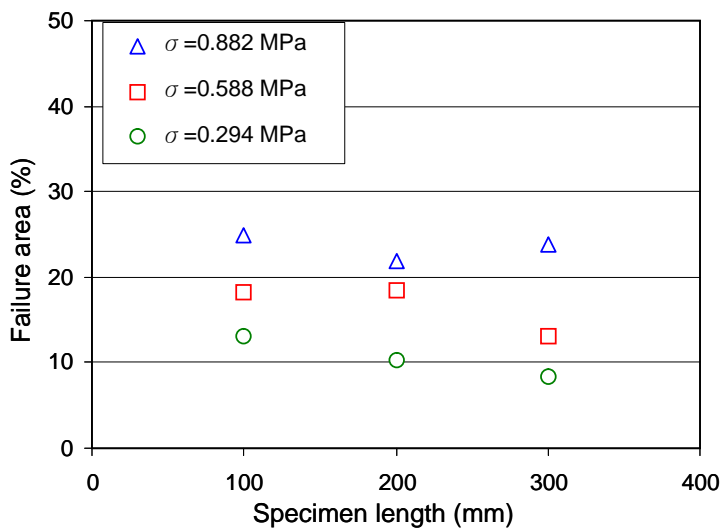
1. The average peak shear strength of the smaller divided joints tends to be higher than that of the original undivided joint, but the strength of each individual small divided joint is not necessarily higher than that of the original joint. The scale effect is less significant for smoother joint surfaces. The roughness of each divided joint surface should be evaluated individually according to its geometry configuration.
2. There is little scale effect on the peak shear strength of the joint specimen whose surface geometry is enlarged or reduced proportionally in both length and height.
3. The peak shear strength of a joint composed of several repeated smaller joint profiles is slightly lower than that of the single smaller joint for rougher joint surfaces ($JRC = 18 \sim 20$, and saw-toothed). No significant strength difference was found for smoother surfaces.
4. The surface conditions after shearing for smaller joint specimens exhibit damaged patterns of small asperities that were not observed for the larger specimens.



(a) Divide joint surfaces



(b) Reduced joint surfaces



(c) Enlarged joint surfaces

Fig. 16 Failure area percentage versus specimen size for the natural joint surfaces

5. The geometry configuration of a joint surface is the main factor in the scale effect on the peak shear strength of rock joints. The geometry configuration should be carefully evaluated in using the Barton's relations for calculating the shear strength of rock joints.

ACKNOWLEDGEMENTS

The authors thank the helps from the personnel in the rock mechanics laboratory and CAM laboratory at National Taiwan University. The modification and improvement of the direct shear test machine were partly supported by the National Science Council, Taiwan, Grant No. NSC89-2211-E-002-055.

REFERENCES

Bandis, S., Lumsden, A. C., and Barton, N. R. (1981). "Experimental studies of scale effects on the shear behaviour of rock joints." *International Journal for Rock Mechanics Min. Sci. and Geomechanics Abstract*, **18**, 1-21.

Barton, N. and Bandis, S. (1982). "Effect of block size on the shear behavior of jointed rock." *Proceedings of the 23rd Symposium on Rock Mechanics*, Berkeley, 739-760.

Barton, N. and Choubey, V. (1977). "The shear strength of rock joints in theory and practice." *Rock Mechanics*, **10**, 1-54.

Brown, E. T., Richards, L. R., and Barr, M. V. (1977). "Shear strength characteristics of the Delabole slates." *Proceedings of the Conf. on Rock Engineering*, Newcastle, 33-51.

Chang, Y. H. (1999). "Preliminary study of scale effect on shear strength of simulated joint surfaces." M.S. Thesis, Department of Civil Engineering, National Taiwan University, Taipei, Taiwan.

Fardin, N., Stephansson, O., and Jing, L. (2001). "The scale dependence of rock joint surface roughness." *International Journal of Rock Mechanics and Mining Sciences*, **38**, 659-669.

Giani, G. P., Ferero, A. M., Passarello, G., and Reinaudo, L. (1992). "Scale effect evaluation on natural discontinuity shear strength." *Proceedings of the Regional Conf. on Fractured and Jointed Rock Masses*, Lake Tahoe, 447-452.

Huang, W. H. (2000). "The scale effect on the shear strength of computer-aid-manufactured joint profiles." M.S. Thesis, Department of Civil Engineering, National Taiwan University, Taipei, Taiwan.

ISRM (1981). *ISRM Suggested Methods for Rock Characterization, Testing and Monitoring*. Commission on Testing Methods, Brown, E.T., editor, Pergamon Press.

Murata, S. and Saito, T. (2003). "A new evaluation method of JRC and its size effect." *Proceedings of the 10th Congress of the International Society of Rock Mechanics*, Johannesburg, 855-858.

Ohnishi, Y. and Herda, H. (1993). "Shear strength scale effect and the geometry of single and repeated rock joints." *Proceedings of the 2nd International Workshop on Scale Effects in Rock Masses*, 167-173.

Ohnishi, Y. and Yoshinaka, R. (1992). "Laboratory investigation of scale effect in mechanical behavior of rock joint." *Proceedings of the Regional Conf. on Fractured and Jointed Rock Masses*, Lake Tahoe, 484-489.

Peng, I. H. (2001). "Geometry factor in scale effect on shear strength of rock joint surfaces." M.S. Thesis, Department of Civil Engineering, National Taiwan University, Taipei, Taiwan.

Pratt, H. R., Black, A. D., and Brace, W. F. (1974). "Friction and jointed quartz diorite." *Proceedings of the 3rd Congress ISRM*, Denver, IIA, 306-310.

Vallier, F., Mitani, Y., Esaki, T., and Boulon, M. (2005). "Rock joints modeling and application to scale effects, improvements." *Proceedings of the 40th U.S. Symposium on Rock Mechanics*, Anchorage, Paper No. 05-737.

